March 2003 • NREL/CP-550-33601

Conference Paper

Predicting Long-Term Performance of Photovoltaic Arrays Using Short-Term Test Data and an Annual Simulation Tool

Preprint

G. Barker
Mountain Energy Partnership
Longmont, Colorado

P. Norton
National Renewable Energy Laboratory

To be presented at the Solar 2003 Conference:
America's Secure Energy
Austin, Texas
June 21–26, 2003

National Renewable Energy Laboratory

1617 Cole Boulevard
Golden, Colorado 80401-3393

NREL is a U.S. Department of Energy Laboratory
Operated by Midwest Research Institute • Battelle • Bechtel

Contract No. DE-AC36-99-GO10337

PREDICTING LONG-TERM PERFORMANCE OF PHOTOVOLTAIC ARRAYS USING SHORT-TERM TEST DATA AND AN ANNUAL SIMULATION TOOL

Greg Barker
Mountain Energy Partnership
13900 North 87th St.
Longmont, CO 80503
GBarker123@aol.com

Paul Norton
National Renewable Energy Laboratory
1617 Cole Blvd.
Golden, CO 80401
Paul_Norton@NREL.gov

ABSTRACT

We present a method of analysis for predicting annual performance of an in-situ photovoltaic (PV) array using short-term test data and an annual simulation tool. The method involves fitting data from a family of I-V curves (depicting current versus voltage) taken from a short-term test (1 to 3 day) of a PV array to a set of polynomial functions. These functions are used to predict the array's behaviour under a wide range of temperatures and irradiances. TRNSYS, [1] driven by TMY2 weather data, is used to simulate the array's behaviour under typical weather conditions. We demonstrate this method by using results from a nominal 630-W array.

1. INTRODUCTION

The manufacturer of a PV module will typically supply data that describe a module's voltage and current characteristics under standard test conditions (I_c = 1000 W/m^2, T_c = 25^{o}C). Often, temperature coefficients for voltage and current are also supplied, which can nominally be used to translate the points on an I-V curve from standard test conditions to other cell temperature conditions. Current output from the module is usually assumed linear with incident irradiance. To predict the performance of an array of modules, the manufacturer's test data for a single module are typically assumed to be accurate for each module in the array, scaling by the number of modules in series and parallel. To account for differences between manufacturers' specifications and actual modules' performance, a "derate factor" is sometimes added in, but there is no quantitative way of establishing this derate factor; it is inserted using engineering judgment and experience. In fact, the difference between nominal and actual performance is rarely as simple as a constant derate factor.

When testing PV arrays in the field, we usually find that the power output of the array is lower than predicted using the above method. This can happen for a number of reasons:

(1) The average module installed in the array is not as efficient as the module tested by the manufacturer because of manufacturing inconsistencies.
(2) The system does not employ a maximum power-point tracking (MPPT) device, and the voltage of the controller setpoint is not always at the maximum power-point voltage. In some systems, we have found that the controller setpoint is never particularly near the maximum power voltage.
(3) Connections between modules and wires to and from the array create voltage drop and power loss in the array.
(4) Solar incidence angle effects result in less collected energy at sharp beam incidence angles.
(5) Performance dependence on the spectral content of irradiance has not been taken into account.

Rather than rely on the manufacturer's module-level data for predicting a PV array's performance, we suggest that the array be tested in-situ over a short period of 1 to 3 days to characterize its behaviour. This characterization can then be used in an annual simulation driven by TMY2 data to predict its behaviour under typical weather conditions. Extrapolating from short-term measured data to long-term performance is a reasonable way to compare the performance of one system to another (i.e., how they compare under typical and identical driving weather conditions).

King et al. [2, 3] previously reported on detailed methods for extrapolating measured data to long-term performance. We simplified their analytical approach and developed a practical short-term field test method. We also added some general correlations to predict certain performance parameters of PVs for which there may be limited information from the manufacturer. In general,

the method involves measuring I-V (current-voltage) curves for the entire array over the period of one clear day (sunrise to sunset) to obtain curves under a range of irradiances and cell temperatures. Five points along the I-V curve — short-circuit, maximum power, open circuit, and two intermediate points — are defined in terms of polynomials as a function of irradiance and back-of-module temperature. For any irradiance and module temperature, the position of these five points on the I-V curve can be calculated and a curve drawn connecting them. An annual simulation such as TRNSYS [1] can then be used to predict power output of the array for every hour of a typical year, given knowledge of the voltage-tracking characteristics of the controller.

In sections 2 through 7 of this paper, we describe in detail the various steps that are taken in starting with data from a short-term test and arriving at a prediction of annual energy production of a PV array.

2. EFFECTIVE IRRADIANCE

The effective irradiance ($I_{c,eff}$) is defined as the equivalent global irradiance that would be falling on the surface of the array if the sun was directly overhead and the array was horizontal. In our approach, the performance of the PV array is expressed in terms of $I_{c,eff}$. The effective irradiance is affected by two phenomena: spectral effects and incidence angle effects.

2.1 Spectral Effects Resulting from Air Mass

Absolute air mass (A_{ma}) is defined as the ratio of mass of atmosphere through which beam radiation passes to the mass it would pass through if the sun were directly overhead. As the air mass increases, the spectral content of irradiance changes. For some PVs, notably amorphous, this has an effect on the efficiency of the PV. King et al. [2, 3] characterized this dependency in the form of a polynomial as a function of A_{ma} for several different types of PV modules. A database containing the values of the polynomial constants are available from the Sandia National Laboratory Web site at http://www.sandia.gov/pv/pvc.htm.

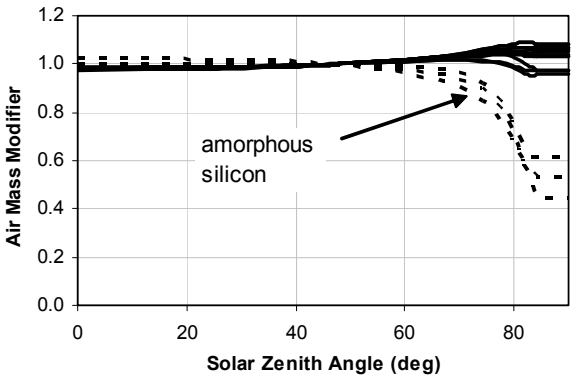

Fig. 1. Air mass modifier as a function of solar zenith angle for all PV modules in the Sandia National Laboratory database. The curves have been limited to the values at solar zenith (84 degrees; air mass = 10) because the correlations blow up at very high air mass values.

The form of the equation for the Air Mass Modifier (M_{Ama}) is as follows:

$$M_{Ama} = a_0 + a_1*A_{ma} + a_2*A_{ma}^2 + a_3*A_{ma}^3 + a_4*A_{ma}^4 \quad \textbf{(1)}$$

The shapes of M_{Ama} as a function of solar zenith angle for all PV modules in the Sandia database are shown in Figure 1.

2.2 Incidence Angle Effects

The incidence angle (θ_i) is the angle between the direction of beam irradiance and a normal to the surface of the PV. With the sun directly overhead and the array horizontal, the incidence angle is zero. As the incidence angle increases, a larger portion of beam radiation is reflected from the glazing surface. King et al. [2,3] characterized this behaviour in the form of a polynomial for several different PV types:

$$M_{\theta i} = b_0 + b_1\theta_i + b_2\theta_i^2 + b_3\theta_i^3 + b_4\theta_i^4 + b_5\theta_i^5 \quad \textbf{(2)}$$

The values of $M_{\theta i}$ for all modules in the Sandia National Laboratory database are shown as a function of incidence angle in Figure 2.

The effective irradiance, which is the irradiance incident on the plane of the array modified by M_{Ama} and $M_{\theta i}$, can then be expressed as:

$$I_{c,eff} = M_{Ama}*(M_{\theta i}*I_b + I_d). \quad \textbf{(3)}$$

Note that the air mass modifier affects both the beam and diffuse components of irradiance, whereas the incidence angle modifier affects only the beam portion. Typically, only the global irradiance in the plane of the array is measured during testing; the split between beam and diffuse can be approximated using an estimate of ground reflectance and correlations for estimating the beam and diffuse components of irradiance. [4,5]

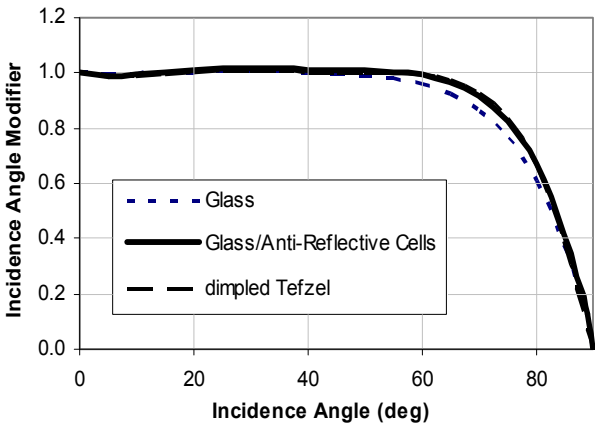

Fig. 2. Incidence angle modifier as a function of incidence angle for all modules in the Sandia database.

3. POSITION OF FIVE POINTS ON THE I-V CURVE

King et al.[2, 3] proposed that under any one set of irradiance and temperature conditions, five points on the I-V curve can be used to define the shape of the curve:

(1) $i = i_{sc}$, $V = 0$

(2) $i = i_x$, $V = 0.5*V_{oc}$

(3) $i = i_{mp}$, $V = V_{mp}$

(4) $i = i_{xx}$, $V = 0.5*(V_{mp}+V_{oc})$

(5) $i = 0$, $V = V_{oc}$

These five points are each characterized as a function of $(I_{c,eff}-I_{c0})$ and $(T_{mod}-T_{mod0})$ according to Equations 4 through 9. We have adopted King's general approach, but simplified the equations somewhat to make them easier to grasp:

$$i_{sc} = i_{sc0}[1+(I_{c,eff}-I_{c0})/I_{c0}][(1+\alpha_{isc}(T_{mod}-T_{mod0})] \quad \textbf{(4)}$$

$$i_x = i_{x0}\{[1+(I_{c,eff}-I_{c0})/I_{c0}] + c_1[1+(I_{c,eff}-I_{c0})/I_{c0}]^2\}[1+\alpha_{ix}(T_{mod}-T_{mod0})] \quad \textbf{(5)}$$

$$i_{mp} = i_{mp0}\{[1+(I_{c,eff}-I_{c0})/I_{c0}] + d_1[1+(I_{c,eff}-I_{c0})/I_{c0}]^2\}[1+\alpha_{imp}(T_{mod}-T_{mod0})] \quad \textbf{(6)}$$

$$i_{xx} = i_{xx0}\{[1+(I_{c,eff}-I_{c0})/I_{c0}] + e_1[1+(I_{c,eff}-I_{c0})/I_{c0}]^2\}[1+\alpha_{ixx}(T_{mod}-T_{mod0})] \quad \textbf{(7)}$$

$$V_{mp} = V_{mp0}+f_1(I_{c,eff}-I_{c0})+f_2(I_{c,eff}-I_{c0})^2 + \beta_{Vmp}(T_{mod}-T_{mod0}) \quad \textbf{(8)}$$

$$V_{oc} = V_{oc0} + g_1(I_{c,eff}-I_{c0}) + g_2(I_{c,eff}-I_{c0})^2 + \beta_{Voc}(T_{mod}-T_{mod0}) \quad \textbf{(9)}$$

4. DETERMINING ANY POINT ON THE CURVE

Using Equations 4 through 9, five points on the I-V curve are defined for any pairing of module temperature and irradiance. The task is then to fit a curve through these five points so that for any voltage between zero and $V_{oc,}$ the current output of the array can be predicted. Luft et al., in work done for TRW, Inc.,[6] proposed an equation form that fits I-V curves quite well:

$$i_{TRW} = i_{sc} * [1 - k_2 * (e^{(V / (k1 * Voc))} - 1)] \quad \textbf{(10)}$$

where:

$$k_1 = (V_{mp} / V_{oc} - 1) / Ln(1 - i_{mp} / i_{sc}) \quad \textbf{(11)}$$

$$k_2 = (1 - i_{mp} / i_{sc}) * e^{(-Vmp / (k1 * Voc))}. \quad \textbf{(12)}$$

Equation 10 is attractive because it involves only the known values of current and voltage at the short-circuit, maximum power, and open-circuit points. Hart and Raghuraman[13] noted, however, that Equation 10 tends to slightly overestimate current as a function of voltage between $V = 0$ and $V = V_{mp}$. To force a more exact fit through the two remaining points (i_x,V_x and i_{xx},V_{xx}) predicted by Equations 5 and 7, we employed the classical single diode model of a photovoltaic module:

$$i = i_L - i_o * (e^{(V + i * Rs) / z)} - 1) - (V + i * R_s) / R_{sh.} \quad \textbf{(13)}$$

In the past, researchers have attempted to define the behaviour of an array under all temperature and irradiance conditions using Equation 13 and the five constants i_L, i_0, R_s, R_{sh}, and z. We have found that this is not a very robust approach and does not fit the array's behaviour well under all conditions. Our approach is to use Equation 13 as an equation form that is a good fit for the five points described by Equations 4 through 9 under a particular pairing of temperature and irradiance conditions (Figure 3). The constants i_L, i_0, R_s, R_{sh}, and z may be completely different for a different temperature or irradiance.

To find the best fit for the five constants in Equation 13, we first reduce the equation so that it has two unknown constants, R_s and z. This is done by recognizing that $i = 0$ at $V = V_{oc}$ and solving for i_L:

$$i_L = V_{oc} / R_{sh} + i_o * (e^{Voc / z} - 1). \quad \textbf{(14)}$$

We can then substitute Equation 14 into Equation 13 and solve for i_o, recognizing that $V = 0$ at $i = i_{sc}$:

$$i_o = (i_{sc}*R_{sh}+i_{sc}*R_s-V_{oc})/R_{sh}/(e^{(Voc / z)} - e^{(Isc * Rs / z)}) \quad \textbf{(15)}$$

Equations 14 and 15 can then be substituted into Equation 13 to solve for R_{sh} , recognizing that $i = i_{mp}$ at $V = V_{mp}$:

$$R_{sh} = [(i_{sc} * R_s - V_{oc}) * (e^{(Voc / z)} - e^{((Vmp + Imp * Rs) / z)}) + (V_{oc} - V_{mp} - i_{mp} * R_s) * (e^{(Voc / z)} - e^{(isc * Rs / z)})] / [i_{mp} * (e^{(Voc / z)} - e^{(isc * Rs / z)}) + i_{sc} * (e^{((Vmp + Imp * Rs) / z)} - e^{(Voc / z)})] \quad \textbf{(16)}$$

Because we have imposed the restrictions that $i = 0$ at $V = V_{oc}$, $V = 0$ at $i = i_{sc}$, and $i = i_{mp}$ at $V = V_{mp}$, the curve described by Equations 13 through 16 will always pass through these three points on the I-V curve. The constants R_s and z are adjusted to obtain the best fit

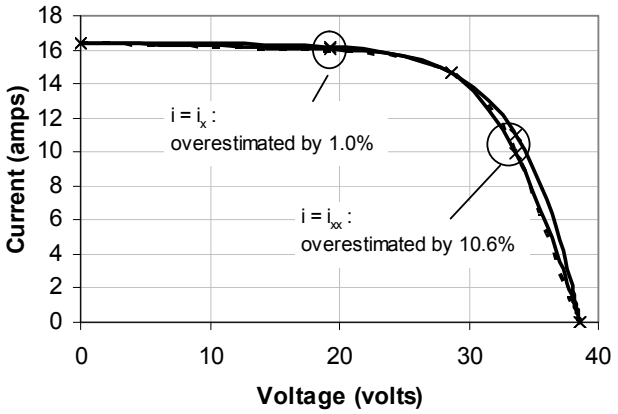

Fig. 3. Example I-V curve showing the five points defined by Equations 4 through 9.

through the two remaining points (i_x, V_x and i_{xx}, V_{xx}) predicted by Equations 5 and 7. The adjustment of R_s and z is made by minimizing the root mean square (RMS) error between the measured and the calculated values of i_x and i_{xx}:

$$E_{rms} = [((i_{x,meas} - i_{x,calc})^2 + (i_{xx,meas} - i_{xx,calc})^2)/2]^{1/2} \quad \textbf{(17)}$$

We performed the minimization of E_{rms} using a routine employing the "Downhill Simplex Method" from Numerical Recipes. [8] We found that the minimization tends to be quite unstable when using Equation 13, predominantly because of its implicit nature (the equation can not be explicitly solved for i). To stabilize the minimization, we substituted i_{TRW} from Equation 10 for i on the right side of Equation 13:

$$i = i_L - i_o * (e^{(V + i_{TRW} * Rs) / z)} - 1) - (V + i_{TRW} * R_s) / R_{sh} \quad \textbf{(18)}$$

Because Equation 10 already predicts i closely, and i only appears on the right side of Equation 18 as part of the product ($i*R_s$), the adjustment of R_s tends to make up for slight errors in i_{TRW}. Occasionally, the minimization routine is unsuccessful in converging on a set of R_s and z that provide a better E_{rms} than Equation 10; in these rare cases, we have reverted to simply using Equation 10 to predict i as a function of V.

Although it is possible to derive a single equation for i with only the two unknown constants R_s and z, the equation is extremely cumbersome. One can alternatively solve for i as a function of V, R_s, and z in 4 steps:

(1) Solve for R_{sh} using R_s, z, and Equation 16

(2) Solve for i_0 using R_{sh} and Equation 15

(3) Solve for i_L using R_{sh}, i_0, and Equation 14

(4) Solve for i using R_{sh}, i_0, i_L, and Equation 18.

5. PREDICTING MODULE TEMPERATURE

Typically, during in-situ testing, it is reasonable to measure the temperature of the back of one or more modules in the array. It is usually not realistic to measure the actual cell temperature because this delicate operation on the back of the module would expose the cells and destroy the integrity of the weatherproof seal, as well as increase the risk of harming the module. King et al.[2, 3] measured both cell and back-of-module temperature for their database of PV modules, and have found that, for a rack-mounted collector, the cell temperature is typically 2-3°C higher than the back-of-module temperature under Standard Rating Conditions. In fact, we need not be concerned with the actual cell temperature in order to calibrate a model for the in-situ array; we propose that all fits be made in respect to the back-of-module temperature.

Predicting the module temperature as a function of outdoor conditions has been the subject of numerous papers, among them King et al.,[2, 3] Del Cueto et al.,[9] Jones et al.,[10] Davis et al.,[14] and Ingersoll.[15] Because of the strong dependence of module temperature on the mounting geometry, we have typically used the approach presented by Ingersoll,[15] which gives methods for estimating module temperature for four different mounting schemes: rack-mount, standoff-mount (small spacing between back of array and roof), direct-mount (back of array directly against roof), and integral mount (array is the roof). Ingersoll proposed a general equation form for calculating T_c:

$$T_c = \frac{(\tau\alpha)I_c - \eta_0 I_c + T_a[h_{cf} + 2\sigma\varepsilon_c\tau_{IR}(1+\cos\beta)T_{sky}T_a^2 + h_{cb} + 4\sigma T_a^3 F_e F_b]}{h_{cf} + 2\sigma\varepsilon_c\tau_{IR}\,T_a^3(1+\cos\beta) + h_{cb} + 4\sigma T_a^3 F_e F_b} \quad \textbf{(19)}$$

and supplied a table of correlations for the calculation of h_{cb}, F_e, and F_b.

The back-of-module temperature, T_{mod}, is assumed to be approximately equal to T_c in the derivation of Equation 19. This is a reasonable assumption for typical PV modules in prediction of T_{mod} for annual simulation. T_{sky} can be estimated using correlations from Martin and Berdahl.[11]

6. PREDICTING ANNUAL PERFORMANCE

We have written a module for TRNSYS[1] for predicting PV array output given the results of a day-long test. Driven by TMY2 weather data, TRNSYS is used to calculate all weather parameters (beam and diffuse insolation, dry-bulb temperature, dewpoint, sky temperature, and wind speed). For each simulation time step (typically 15-minute), a Power-Voltage curve is generated using Equations 1, 2, 4, 5, 6, 7, 8, and 9 and the procedure described in Section 4. Equation 19 is used to predict module temperature. For each time step, then, the power output of the array can be predicted at any voltage.

Typically, we report the maximum possible power output ($V = V_{mp}$) and the actual expected output. In our field tests to date, most systems have either not employed a maximum power-point tracking (MPPT) device, or the MPPT has not operated properly. In typical battery-storage systems, the voltage across the array is equal to the voltage across the battery bank. In these cases, TRNSYS is used to simulate the battery voltage for each time step; this voltage is used to calculate the PV array output for this time step. We have encountered more than one system where the battery voltage was not well-matched with the PV array; the battery voltage was very different than V_{mp}, resulting in lower power output than would be expected if good MPPT were employed.

TABLE 1. M_{AMA} COEFFICIENTS FOR EIGHT CELL MATERIALS

Cell Material	a_0	a_1	a_2	a_3	a_4
Monocrystalline Silicon (c-Si)	1.007493	-2.18335E-02	1.68364E-02	-2.61715E-03	1.21716E-04
Multicrystalline Silicon (mc-Si)	1.002933	-1.38577E-02	1.30445E-02	-2.23131E-03	1.11179E-04
2-Junction Amorphous Silicon (2-a-Si)	0.956028	7.80442E-02	-3.75356E-02	3.56222E-03	-9.91272E-05
3-Junction Amorphous Silicon (3-a-Si)	0.947585	1.04304E-01	-5.88808E-02	7.27597E-03	-2.84873E-04
EFG Multicrystalline Silicon (EFG mc-Si)	1.006921	-2.02301E-02	1.56043E-02	-2.40634E-03	1.11512E-04
Copper Indium Diselenide (CIS)	1.002934	-1.34724E-02	1.25627E-02	-2.13104E-03	1.06505E-04
Cadmium Telluride (CdTe)	1.002757	-1.50992E-02	1.49883E-02	-2.78758E-03	1.41854E-04
Multicrystalline Silicon Film	0.993985	4.45904E-03	2.46337E-03	-9.71569E-04	6.46083E-05

7. GENERALIZING FOR MODULE TYPES NOT IN THE SANDIA DATABASE

Although the Sandia database includes more than 100 module types, it is not uncommon to test an array of modules that are not included in the database. In this case, the coefficients for M_{Ama} and $M_{\theta i}$ are not known (Equations 1 and 2). Fortunately, by examining the Sandia database one can see that, if there is some knowledge of the cell and glazing materials, a reasonable estimate of the coefficients can be made. M_{Ama} is largely a cell material effect; we have condensed this effect into eight categories:

(1) Monocrystalline Silicon (c-Si)
(2) Multicrystalline Silicon (mc-Si)
(3) 2-Junction Amorphous Silicon (2-a-Si)
(4) 3-Junction Amorphous Silicon (3-a-Si)
(5) EFG Multicrystalline Silicon (EFG mc-Si)
(6) Copper Indium Diselenide (CIS)
(7) Cadmium Telluride (CdTe)
(8) Multicrystalline Silicon Film.

The coefficients for Equation 1 are given in Table 1 for each of the eight cell material categories. Similarly, incidence angle behaviour can be generalized into three glazing categories:

(1) Smooth Glass
(2) Smooth Glass with Anti-Reflective Coating on Cells
(3) Dimpled Tefzel.

The coefficients for Equation 2 are given in Table 2 for each of the three glazing categories.

Finally, sometimes the temperature coefficients α_{isc}, β_{Voc}, α_{imp}, β_{Vmp}, α_{ix}, and α_{ixx}, are difficult to determine from a day-long test of an array, particularly the temperature coefficients of current, which are usually very small. When a coefficient is not well determined from a data set using Equations 4 through 9, we like to refer to the manufacturer's data. Coefficients α_{imp}, β_{Vmp}, α_{ix}, and α_{ixx} are typically not provided by the manufacturer, although usually α_{isc} and β_{Voc} are provided. Again referring to the Sandia database of coefficients for different modules, we can predict α_{imp}, β_{Vmp}, α_{ix}, and α_{ixx} for a module with known coefficients α_{isc} and β_{Voc}. We have defined the coefficients r_α and r_β, such that:

$$\alpha_{imp} = r_\alpha \alpha_{isc} \quad \textbf{(20)}$$

$$\beta_{Vmp} = r_\beta \beta_{Voc} \quad \textbf{(21)}$$

By reviewing the Sandia database, we found that the ratios r_α and r_β are more easily generalized by cell material than are α_{imp} and β_{Vmp}. In Table 3, we give the average values of r_α and r_β for eight different cell material categories.

King[2,3] recommended the following equations for estimating α_{ix} and α_{ixx} :

$$\alpha_{ix} = 0.5(\alpha_{isc} + \alpha_{imp}) \quad \textbf{(22)}$$

$$\alpha_{ixx} = \alpha_{imp}. \quad \textbf{(23)}$$

TABLE 2. $M_{\theta i}$ COEFFICIENTS

Value	**Smooth Glass**	**Smooth Glass / Anti-Reflective Cells**	**Dimpled Tefzel**
b_0	1.0	1.0	1.0
b_1	- 3.3101E-03	- 4.6445E-03	- 4.5158E-03
b_2	4.1289E-04	5.8607E-04	5.2488E-04
b_3	- 1.6280E-05	- 2.3108E-05	- 2.0791E-05
b_4	2.6740E-07	3.7843E-07	3.5011E-07
b_5	-1.6432E-09	-2.2515E-09	-2.1457E-09

TABLE 3. TEMPERATURE COEFFICIENT RATIOS (r_α and r_β)

Cell Material	r_α	r_β
Monocrystalline Silicon (c-Si)	-1.349	1.019
Multicrystalline Silicon (mc-Si)	-0.362	1.016
2-Junction A- Silicon (2-a-Si)	1.566	0.802
3-Junction A- Silicon (3-a-Si)	1.382	0.528
EFG MC Silicon (EFG mc-Si)	0.247	1.043
Copper Indium Diselenide (CIS)	34.615	0.835
Cadmium Telluride (CdTe)	-6.508	0.880
Multicrystalline Silicon Film	0.009	0.975

8. CASE STUDY

As an example of how to implement the technique described in this paper, we present the results of a short-term test on a rack-mounted PV array in Golden, Colorado. The test was performed from 11:00 AM to 5:00 PM on June 28, 2001. The array description is given in Table 4. Insolation varied from about 100 to 950 W/m^2, with module temperatures ranging from about 30°C to 55°C. A total of 24 I-V traces were made, once every 15 minutes. The P-V curves are shown in Figure 4.

Applying Equations 4 through 9 to the data set, we performed a linear least-squares regression on each of the six equations to determine each coefficient. Temperature coefficients for currents were not calculated from regression, as these are very small numbers and are, therefore, difficult to determine from a limited data set such as this one.

Table 5 provides the goodness of fit for the six regressions that fit Equations 4 through 9. To compare the parameters at Standard Rating Conditions to data provided by the manufacturer, we multiply voltages and voltage coefficients by the number of modules in series. Currents are multiplied by the number of modules in parallel. This comparison is made in Table 6.

TABLE 4. DESCRIPTION OF TESTED ARRAY

Module Type	Seimens SM55, mc-Si
Number of modules in series/string	2
Number of strings	6
Array Slope	40 degrees from horizontal
Array Azimuth	due south
Array nominal rating	631.5 W

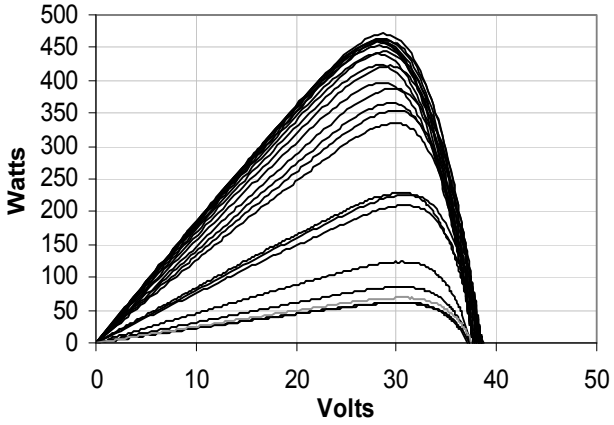

Fig. 4. Power-Voltage curves taken every 15 minutes from 11:00 AM to 5:00 PM.

The type of module in this array can be found in the Sandia database, so coefficients for Equation 1 and Equation 2 were taken from that source.

Annual TRNSYS simulations of the array using TMY2 data for Boulder, Colorado, give the results shown in Table 7. We simulated perfect MPPT and fixed voltage to demonstrate the performance that could be gained by replacing the currently installed fixed-voltage controller with a MPPT. The results show that under the fixed-voltage scenario, the annual energy delivery is about 8.5% lower than would have been expected using published module parameters and 18.8% lower under the MPPT scenario.

One "reality check" we like to make is to infer a wiring resistance from the measured and manufacturer's parameters at the maximum power point. If all of the voltage difference between V_{mp0} (measured) and V_{mp0} (manufacturer) is due to wiring resistance, then the resistance is approximately as follows:

$$R_{wiring} = (V_{mp0,man} - V_{mp0,meas})/i_{mp0,man.} \quad \textbf{(24)}$$

From Table 6, we obtain the following:

$$R_{wiring} = (34.62\text{-}30.34)/18.24 = 0.235 \text{ ohms.} \quad \textbf{(25)}$$

TABLE 5. REGRESSION STATISTICS

Eq. No.	*For Determining*	*RMS error*	*Units*
4	i_{sc}	0.115	amps
5	i_x	0.099	amps
6	i_{mp}	0.099	amps
7	i_{xx}	0.112	amps
8	V_{mp}	0.130	volts
9	V_{oc}	0.146	volts

TABLE 6. PARAMETERS FOR ARRAY AT SRC

Parameter	*Published*	*Measured*	*Difference*	*Units*
i_{sc}	19.86	19.41	-0.45	amps
i_{mp}	18.24	16.97	-1.27	amps
V_{mp}	34.62	30.34	-4.28	volts
P_{mp}	631.5	514.9	-116.6	watts
V_{oc}	42.80	40.80	-2.00	volts
β_{Voc}	-0.16700	-0.10616	+0.06084	V/°C

This is a plausible number for the wiring in the array. If, for example, we arrived at a number that was an order of magnitude larger, we would want to look for problems in the measurements, regressions, or the array itself.

Finally, as a cursory check of Equation 19 for calculating module temperature, we compared measured and modeled module temperature during the test. The model predicts the module temperature with an RMS error of about 7% of the mean for this data set.

9. CONCLUSIONS

The procedures outlined in this paper provide a method of predicting the long-term performance of an in-situ PV array from data taken during a day-long field test. Detailed analysis is provided demonstrating the use of the approach for a single test case. The regression equations used to predict key parameters as a function of ambient conditions fit the data well for our test case.

10. FUTURE WORK

The accuracy of the method needs to be demonstrated in three ways:

(1) Compare long-term measured performance data to predictions using the model provided by this method and actual measured weather data.

(2) Compare parameter predictions (i_{sc0}, i_{x0}, i_{xx0}, i_{mp0}, V_{mp0}, V_{oc0}) from tests performed under different weather conditions (i.e., summer and winter).

(3) Compare I-V curves measured under one set of conditions (e.g., summer) to curves predicted using test results under different conditions (e.g., winter).

TABLE 7. TRNSYS SIMULATION RESULTS

Parameters Used	**Array Voltage**	**Annual DC Energy Delivered (kWh/yr)**
Published	26.8	72.1
Published	MPPT	89.0
Measured	26.8	66.0
Measured	MPPT	72.3

NOMENCLATURE

Symbol	*Description*	*Units*
a	constant in T_{mod} Equation 19	
b	constant in T_{mod} Equation 19	
c_1	constant #1 in i_x polynomial fit	
c_h	coefficient for h_c	
d_1	constant #1 in i_{mp} polynomial fit	
e_1	constant #1 in i_{xx} polynomial fit	
E_{rms}	RMS error between measured and calculated values of i_x and i_{xx}	amps
F_e	back panel surface emissivity factor	
F_b	back panel surface configuration factor	
f_1	constant #1 in V_{mp} polynomial fit	V-m^2/W
f_2	constant #2 in V_{mp} polynomial fit	V-m^4/W^2
g_1	constant #1 in V_{oc} polynomial fit	V-m^2/W
g_2	constant #2 in V_{oc} polynomial fit	V-m^4/W^2
h_{cf}	convective heat-transfer coefficient for array front surface	W/m^2-C
h_{cb}	convective heat-transfer coefficient for array back surface	W/m^2-C
I_c	incident solar radiation	W/m^2
$I_{c,eff}$	effective incident solar radiation	W/m^2
I_{c0}	incident solar radiation at SRC	W/m^2
I_{dh}	total diffuse horizontal radiation	
I_h	total insolation, horizontal surface	
i	current output of array	amps
i_L	"light current" for single diode model	
i_{mp}	current at maximum power point	amps
i_{mp0}	current at max. power point at SRC	amps
$i_{mp0,man}$	current at maximum power point at SRC (manufacturer)	amps
i_o	"diode current" for single diode model	amps
i_{sc}	short-circuit current of array	amps
i_{sc0}	short-circuit current of array at SRC	amps
i_{TRW}	current predicted using Equation 10 (TRW equation)	amps
i_x	current output of array at V = 0.5*V_{oc}	amps
i_{x0}	current output of array at V = 0.5*V_{oc} at SRC	amps
i_{xx}	current output of array at V = 0.5*(V_{mp}+V_{oc})	amps
i_{xx0}	current output of array at V = 0.5*(V_{mp}+V_{oc}) at SRC	amps
$i_{x,meas}$	measured value of i_x	amps
$i_{x,calc}$	calculated value of i_x using Equations 14 through 16 and 18	amps
$i_{xx,meas}$	measured value of i_{xx}	amps

$i_{xx,calc}$	calculated value of i_{xx} using Equations 14 through16 and 18	amps
k_1	coefficient in the TRW equation	
k_2	coefficient in the TRW equation	
r_α	ratio of α_{imp} to α_{isc}	
R_s	series resistance, single diode model	ohms
R_{sh}	shunt resistance, single diode model	ohms
R_{wiring}	total resistance of array wiring	ohms
r_β	ratio of β_{Vmp} to β_{Voc}	
SRC	Standard Rating Conditions (I_c = 1000 W/m^2, Tc = 25 ^{o}C)	
T_a	ambient air temperature	°C
T_c	cell temperature	°C
T_{c0}	cell temperature at SRC	°C
T_{mod}	back-of-module temperature	°C
T_{mod0}	back-of-module temperature at SRC	°C
T_{sky}	effective black-body sky temperature	Kelvin
V	voltage across array	volts
V_{oc}	array open-circuit voltage	volts
V_{oc0}	array open-circuit voltage at SRC	volts
V_{mp}	voltage at maximum power point	volts
$V_{mp0,man}$	voltage at maximum power point (manufacturer's data)	volts
$V_{mp0,meas}$	voltage at maximum power point (measured data)	volts
V_{mp0}	voltage at maximum power point at SRC	volts
z	curve-fitting parameter for single diode model	
α_{imp}	temperature coefficient for i_{mp}	1/deg C
α_{isc}	temperature coefficient for i_{sc}	1/deg C
α_{ix}	temperature coefficient for i_x	1/deg C
α_{ixx}	temperature coefficient for i_{xx}	1/deg C
β	slope of array from horizontal	deg
β_{Vmp}	temperature coefficient for V_{mp}	V/deg C
β_{Voc}	temperature coefficient for V_{oc}	V/deg C
ε_c	emissivity of cell material	
τ_{IR}	IR transmittance of glazing material	
γ	temperature coefficient of efficiency	
η_0	array efficiency at SRC	
σ	Stefan-Boltzman constant	W/m^2-K^4
$(\tau\alpha)$	transmittance-absorptance product for solar radiation	

REFERENCES

(1) Klein, S., et al., TRNSYS: A Transient System Simulation Program – Reference Manual, Solar Energy Laboratory, University of Wisconsin, 1996

(2) King, D.L., Photovoltaic Module and Array Performance Characterization Methods for All System Operating Conditions, Proceeding of NREL/SNL Photovoltaics Program Review Meeting, November 18-22, 1996, Lakewood, CO, AIP Press, New York, 1997

(3) King, D.L., Kratochvil, J.A., Boyson, W.E., Field Experience with a New Performance Characterization Procedure for Photovoltaic Arrays, presented at the 2nd World Conference and Exhibition on PV Solar Energy Conversion, Vienna, Austria, 1998

(4) Erbs, D.G., Methods For Estimating the Diffuse Fraction of Hourly, Daily, and Monthly Average Global Solar Radiation, Masters Thesis Mechanical Engineering, Univ. Wisconsin, Madison, 1980

(5) Hay, J.E., and Davies, J.A., Calculation of the Solar Radiation Incident On An Inclined Surface, Proceedings First Canadian Solar Radiation Workshop, pp. 59-72, 1980

(6) Luft, W., Barton, J.R., and Conn, A.A., Multifaceted Solar Array Performance Determination, TRW Systems Group, Redondo Beach, CA, February 1967

(7) Duffie, J., and Beckman, W., Solar Engineering of Thermal Processes, 2nd Edition, John Wiley & Sons, Inc., New York, 1991

(8) Press, W., Flannery, B.P., Teukolsky, T., and Vetterling, W. T., Numerical Recipes, Cambridge University Press, page 292, 1989

(9) del Cueto, J.A., Model for the Thermal Characteristics of Flat-Plate Photovoltaic Modules Deployed at Fixed Tilt, Conference Record of the Twenty-Eighth IEEE Photovoltaic Specialists Conference, 15-22 September, Anchorage, Alaska, 2000

(10) Jones, A.D., and Underwood, C.P., A Thermal Model for Photovoltaic Systems, Solar Energy, Vol. 70, (4), pp. 349-359, 2001

(11) Martin, M., and Berdahl, P., Characteristics of Infrared Sky Radiation in the United States, Solar Energy, Vol. 33, pp. 241-252, 1984

(12) Kasten C., Solar Energy, Vol. 24, pp 177-189

(13) Hart, G.W., and Raghuraman, P., Electrical Aspects of Photovoltaic System Simulation, Massachusetts Institute of Technology, Lincoln Laboratory, Lexington, MA, 1982

(14) Davis, M.W., Fanney, A.F., and Dougherty, B.P., Prediction of Building Integrated Photovoltaic Cell Temperatures, Proceedings of Solar Forum 2001, ASME, April 21-25, 2001

(15) Ingersoll, J.G., Simplified Calculation of Solar Cell Temperatures in Terrestrial Photovoltaic Arrays, Journal of Solar Energy Engineering, Vol. 108, pp. 95-101, 1986

REPORT DOCUMENTATION PAGE

Form Approved
OMB NO. 0704-0188

1. AGENCY USE ONLY (Leave blank)	2. REPORT DATE	3. REPORT TYPE AND DATES COVERED
	March 2003	Conference Paper

4. TITLE AND SUBTITLE
Predicting Long-Term Performance of Photovoltaic Arrays Using Short-Term Test Data and an Annual Simulation Tool: Preprint

5. FUNDING NUMBERS

6. AUTHOR(S)
G. Barker and P. Norton

7. PERFORMING ORGANIZATION NAME(S) AND ADDRESS(ES)
National Renewable Energy Laboratory
1617 Cole Blvd.
Golden, CO 80401-3393

8. PERFORMING ORGANIZATION REPORT NUMBER
NREL/CP-550-33601

9. SPONSORING/MONITORING AGENCY NAME(S) AND ADDRESS(ES)

10. SPONSORING/MONITORING AGENCY REPORT NUMBER

11. SUPPLEMENTARY NOTES

12a. DISTRIBUTION/AVAILABILITY STATEMENT
National Technical Information Service
U.S. Department of Commerce
5285 Port Royal Road
Springfield, VA 22161

12b. DISTRIBUTION CODE

13. ABSTRACT *(Maximum 200 words)*
We present a method of analysis for predicting annual performance of an in-situ photovoltaic (PV) array using short-term test data and an annual simulation tool. The method involves fitting data from a family of I-V curves (depicting current versus voltage) taken from a short-term test (1 to 3 day) of a PV array to a set of polynomial functions. These functions are used to predict the array's behaviour under a wide range of temperatures and irradiances. TRNSYS, driven by TMY2 weather data, is used to simulate the array's behaviour under typical weather conditions. We demonstrate this method by using results from a nominal 630-W array.

14. SUBJECT TERMS
Photovoltaic; long-term performance; short-term testing; simulation tools; PV

15. NUMBER OF PAGES

16. PRICE CODE

17. SECURITY CLASSIFICATION OF REPORT	18. SECURITY CLASSIFICATION OF THIS PAGE	19. SECURITY CLASSIFICATION OF ABSTRACT	20. LIMITATION OF ABSTRACT
Unclassified	Unclassified	Unclassified	UL